YALE
PEABODY
MUSEUM

JOURNAL OF MARINE RESEARCH

The *Journal of Marine Research,* one of the oldest journals in American marine science, published important peer-reviewed original research on a broad array of topics in physical, biological, and chemical oceanography vital to the academic oceanographic community in the long and rich tradition of the Sears Foundation for Marine Research at Yale University.

An archive of all issues from 1937 to 2021 (Volume 1–79) are available through EliScholar, a digital platform for scholarly publishing provided by Yale University Library at https://elischolar.library.yale.edu/.

Requests for permission to clear rights for use of this content should be directed to the authors, their estates, or other representatives. The *Journal of Marine Research* has no contact information beyond the affiliations listed in the published articles. We ask that you provide attribution to the *Journal of Marine Research.*

Yale University provides access to these materials for educational and research purposes only. Copyright or other proprietary rights to content contained in this document may be held by individuals or entities other than, or in addition to, Yale University. You are solely responsible for determining the ownership of the copyright, and for obtaining permission for your intended use. Yale University makes no warranty that your distribution, reproduction, or other use of these materials will not infringe the rights of third parties.

Journal of
MARINE RESEARCH

Mean energy balance in the tropical Pacific Ocean

by Jaclyn N. Brown[1,2] and Alexey V. Fedorov[1]

ABSTRACT

The maintenance of the ocean general circulation requires energy input from the wind. Previous studies estimate that the mean rate of wind work (or wind power) acting on the surface currents over the global ocean amounts to 1.1 TW (1 TW $= 10^{12}$ Watts), though values remain highly uncertain. By analyzing the output from a range of ocean-only models and data assimilations, we show that the tropical Pacific Ocean contributes around 0.2 to 0.4 TW, which is roughly half of the total tropical contribution. Not only does this wind power represent a significant fraction of the total global energy input into the ocean circulation, it is also critical in maintaining the east-west tilt of the ocean thermocline along the equator. The differences in the wind power estimates are due to discrepancies in the wind stress used to force the models and discrepancies in the surface currents the models simulate, particularly the North Equatorial Counter Current and the South Equatorial Current. Decadal variations in the wind power, more prominent in some models, show a distinct decrease in the wind power in the late 1970s, consistent with the climate regime shift of that time and a flattening of the equatorial thermocline. We find that most of the wind power generated in the tropics is dissipated by friction in the mixed layer and in zonal currents with strong vertical and horizontal shears. Roughly 10 to 20% of the wind power (depending on the model) is transferred down the water column through vertical buoyancy fluxes to maintain the thermocline slope along the equator. Ultimately, this fraction of the wind power is dissipated by a combination of vertical and horizontal diffusion, energy advection out of the tropics, and damping by surface heat fluxes. Values of wind power generated in the tropical Pacific by coupled general circulation models are typically larger than those generated by ocean-only models, and range from 0.3 to 0.6 TW. Even though many models simulate a 'realistic' climate in the tropical ocean, their energy budgets can still vary greatly from one

1. Department of Geology and Geophysics, Yale University, P.O. Box 208109, New Haven, Connecticut, 06511, U.S.A.
2. Present address: Centre for Australian Weather and Climate Research, CSIRO Marine and Atmospheric Research, GPO Box 1538, Hobart, Tasmania, Australia 7001. *email: jaci.brown@csiro.au*

model to the next. We argue that a correct energy balance is an essential measure of how well the models represent the actual ocean physics.

1. Introduction

Energy input to the ocean by the wind stress, or wind power, is the main source of mechanical energy for the oceanic general circulation (e.g. Wunsch and Ferrari, 2004; Huang, 2004). It is estimated that globally the wind power supplies approximately 1.1 TW (1 Terawatt $= 10^{12}$ Watts) to the ocean circulation (Huang *et al.*, 2006). The largest source of this wind power occurs in the Southern Ocean where the strong westerly winds drive the Antarctic Circumpolar Current. The tropical Pacific is the next largest source because of the strong trade winds and zonal currents. The tropical oceans are also responsible for most of the interannual variability in the global signal of the wind power (Huang *et al.*, 2006).

The ocean energetics in the tropics describes the relationship between wind power, buoyancy power, and the available potential energy (Goddard and Philander, 2000; Fedorov *et al.*, 2003; Fedorov, 2007). When the wind vector projects positively onto the ocean surface current (i.e. the wind blows in the same direction as the current), the mechanical energy of the ocean is increased. This process represents a transfer of wind power from the atmosphere to the ocean. When the winds blow in the opposite direction, the result is to remove energy from the system (negative wind power).

The physical meaning of wind power is the rate of wind work, or more specifically, the rate of the work of the wind stress on ocean currents, and it is measured in Watts. For the sake of brevity, previous studies sometimes referred to this variable as work done by the winds or simply wind work (e.g. Fedorov, 2007; Wunsch, 1998). Here, we will follow the strict physical definition and refer to it as wind power.

A significant fraction of the wind power is converted to buoyancy power. Buoyancy power causes vertical movements in the isopycnals and affects the rate of change of available potential energy in the system. In the tropical Pacific Ocean, as we are going to show, the mean available potential energy is primarily a measure of the mean thermocline slope along the equator. Therefore, in the tropical Pacific, there is a direct connection between the wind power at the ocean surface and the mean slope of the thermocline.

Existing estimates of wind power over the global ocean have large uncertainty (Wunsch, 1998; Huang *et al.*, 2006). Ideally, to calculate wind power accurately, well-resolved datasets of winds and surface currents are needed. However, direct observations of surface currents are sparse, while indirect estimates of surface velocity using sea surface heights are inaccurate, especially in the vicinity of the equator. The overall energy balance is even harder to estimate, since it requires accurate information on subsurface variables, such as vertical velocity and density.

In this study, we determine the mean wind power acting on the tropical Pacific Ocean and its effect on available potential energy, by comparing a number of different sources, including ocean-only models and data assimilations. We explore what factors determine the values of the mean wind power, and how the mean wind power changes over decadal

timescales. Further, we estimate the proportion of wind power that is converted to buoyancy power, which is then used to re-supply energy lost to dissipation and is essential for maintaining the slope of the thermocline. We will compare these results with the results from several coupled models from the Program for Climate Model Diagnosis and Intercomparison (PCMDI) database including some from the Intergovernmental Panel on Climate Change Fourth Assessment Report (IPCC AR4).

Our estimates of the mean wind power in ocean-only models and ocean data assimilations range from 0.2 to 0.4 TW over the tropical Pacific, which represent a substantial fraction of the previous estimated global value of 1.1 TW. These numbers would increase further, if the Atlantic and Indian oceans are also taken into consideration. The discrepancies in our estimates of the wind power can be accounted for by a combination of differences in the wind stress used to force the models and the simulated structure of the ocean surface currents.

Coupled models tend to overestimate the mean wind power with values nearing 0.6 TW, which is related primarily to excessively strong winds produced by the models. In turn, too strong wind power leads to larger buoyancy power, which supports a steeper thermocline in some of the coupled models.

Finally, we find that the wind power in the tropical Pacific is subject to significant decadal variations, especially related to the climate shift of the late 1970s (e.g. Guilderson and Schrag, 1998; Fedorov and Philander, 2000). Thus, our results indicate that accurate estimates of the global wind power, and hence of the net wind work on the ocean general circulation, require a careful consideration of the tropical ocean.

2. The energy balance for the tropical ocean

The energy balance for the tropical basin can be written in terms of changes in the kinetic (K) and available potential energy (APE or E for brevity)

$$\frac{\partial K}{\partial t} = W - B - Dissipation$$

$$\frac{\partial E}{\partial t} = B - Dissipation.$$

(1)

Here, W is the wind power and B is the buoyancy power (also referred to as the conversion of kinetic to potential energy (Wunsch and Ferrari, 2004)). Dissipation refers to the loss of power due to dissipative processes and energy loss at the boundaries of the tropical basin.

We focus on the Pacific region between 15S to 15N and 140E to the coast of the Americas. This region is chosen to capture the important ENSO dynamics and minimize other climatic contributions. For example, the dominant wind power signal is contained within this box, however the noise-prone features due to western boundary currents have been excluded. Further comprehensive discussion of why this region is chosen can be

found in Brown and Fedorov (2008). A full analysis of these equations is given in the Appendix.

For a steady state, the time dependent terms on the left-hand side of (1) vanish. The net wind power, W, is positive, providing a source of energy in the kinetic energy equation. Mean wind power (in Watts) is calculated as

$$W = \iint \langle \tau v \rangle dxdy \approx \iint \langle \tau^x u \rangle dxdy \qquad (2)$$

where $\tau = (\tau^x, \tau^y)$ is the wind stress, and $v = (u, v)$ is the horizontal velocity measured in (2) at the ocean surface. The brackets indicate a time average and the integration is done over our region of interest (Fig. 1a). The meridional component of the wind power (meridional wind stress multiplied by meridional currents) accounts for only 4% of the global total (Wunsch, 1998) and can be neglected.

In addition, the mean wind power can be approximated as the product of the mean wind stress and the mean surface velocity (Wunsch, 1998).

$$\iint \langle \tau^x u \rangle dxdy \approx \iint \langle \tau^x \rangle \langle u \rangle dxdy. \qquad (3)$$

We will use this approximate relationship to explore the separate roles of the wind stress and surface current in determining the total wind power.

Once the wind power is applied to the ocean, part of it is dissipated, and part is converted to buoyancy power, as described by Eq. (1). The mean buoyancy power is defined as

$$B = \iiint \langle g\tilde{\rho}w \rangle dxdydz \qquad (4)$$

where g is gravity, w is the vertical velocity and, $\tilde{\rho}$ is the density anomaly defined as the difference between potential density $\rho = \rho(x, y, z, t)$ and a hydrostatically stable density profile $\rho = \rho*(z)$. That is, $\tilde{\rho} = \rho - \rho*$, with $\rho*$ being a horizontal and time average. The buoyancy power is responsible for the conversion of kinetic energy into potential energy.

The mean available potential energy (in Joules), APE or E for brevity, can be written in terms of potential density ρ according to Oort *et al.* (1989) as

$$E = \iiint \frac{1}{2} \left\langle \frac{\tilde{\rho}^2}{S^2} \right\rangle dxdydz \qquad (5)$$

where $S^2 = |(1/g)(d\rho*/dz)|$ is a stability factor related to the buoyancy frequency. A derivation of this definition of APE and its limitations can be found in Huang (1998). The APE is a measure of the density perturbation from a flat horizontal background. In the
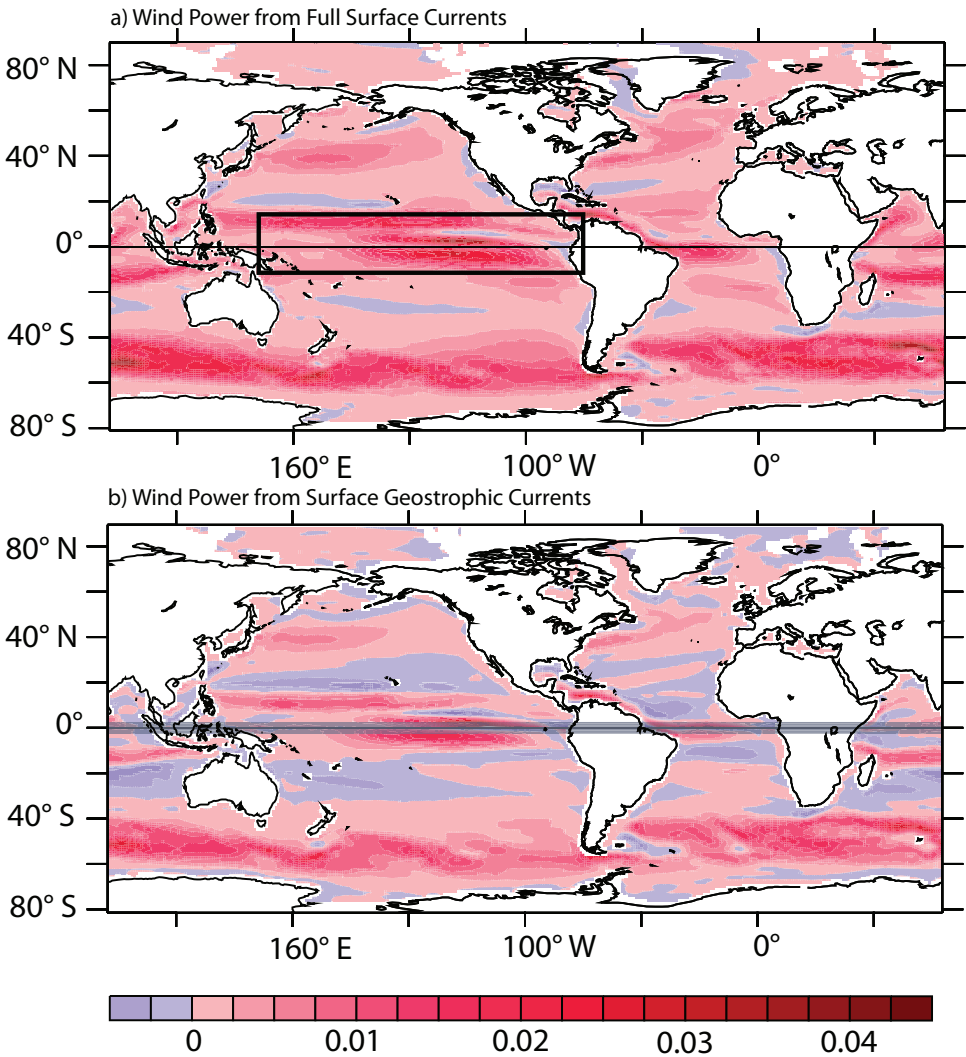
Figure 1. Mean wind power per unit area, obtained as a time average of the product $u\tau^x$ using the full zonal surface velocity (top panel) and only its geostrophic component (bottom panel), from MOM4 calculations. The black box indicates the boundaries of the tropical Pacific as used in our study (contributions from the Gulf of Carpentaria and the Caribbean are removed from the calculations).

tropical Pacific, the largest perturbation is due to the zonal thermocline slope. Therefore, the APE is primarily a measure of the tilt of the thermocline along the equator.

When calculating the wind power, the surface velocity can be separated into two components, the geostrophic and ageostrophic (primarily Ekman)

$$u = u_g + u_{ag}. \tag{6}$$

Neglecting a narrow equatorial strip, Huang *et al.* (2006) estimated that the global wind power from geostrophic currents is 0.84 TW (averaged between 1993 and 2003), but increases to 1.16 TW if the full surface current is used. It has been argued previously (Wang and Huang, 2004; Weijer and Gille, 2005) that, away from the equator, the contribution to the wind power from ageostrophic velocity is largely dissipated in the ocean mixed layer.

In the equatorial region, however, the separation of the flow into the geostrophic and ageostrophic components is not possible. Therefore, the wind power must be calculated using the full surface velocity. In fact, we will show that changes in the APE of the tropical basin critically depend on the wind power generated in the equatorial band and so the equatorial region cannot be neglected.

3. Models, data assimilations and observations

In this study, we will use the output of four ocean-only models, two ocean data assimilation products and six simulations by coupled general circulation models (GCM):

The ocean-only models are

1. Modular Ocean Model (MOM4), forced with NCEP/NCAR reanalysis winds.

2. Parallel Ocean Program (POP), forced with a version of NCEP/NCAR reanalysis winds, adjusted for satellite products (Maltrud and McClean, 2005).

3. The NEMO/ORCA05 model, or simply ORCA.

Two different numerical simulations with the ORCA model are analyzed, one with the wind forcing from the NCEP/NCAR reanalysis (ORCAa) and the other based on ERA-40 winds (ORCAb).

The two data assimilations are

1. Estimating the Circulation and Climate of the Ocean (ECCO).

2. Global Ocean Data Assimilation System (GODAS).

The coupled GCM simulations are from the archive of coupled climate results organized by the Program for Climate Model Diagnosis and Intercomparison (PCMDI) including some that appeared in the Intergovernmental Panel on Climate Change (IPCC) Fourth Assessment Report (AR4). In each case we have taken the 20th century scenario, known as 20c3m. For detailed documentation and validation of these models, see Meehl *et al.* (2007) and the PCMDI web site at http://esg.llnl.gov/portal.

More detailed information on the models and data assimilations is summarized in Table 1. Our results will also be compared with observations where applicable, in particular, the ERA-40 wind stress (Uppala *et al.*, 2005) and the observational data on tropical ocean currents processed by Johnson *et al.* (2002).

Table 1. Details of the ocean-only models, data assimilations and coupled models analyzed in this study, including the period of the calculations, the ocean resolution near the equator, and where relevant, the wind stress product used to force the model.

Model/data product	Simulation period used	Oceanic resolution (at equator)	Wind stress	Reference
Ocean Models				
ORCAa, IPSL/LOCEAN	1964–2000	$0.5° \times 0.5°$	NCEP/NCAR reanalysis	Barnier *et al.* (2006)
ORCAb, IPSL/LOCEAN	1964–2000	$0.5° \times 0.5°$	ERA40	Barnier *et al.* (2006)
MOM4, GFDL	1960–2001	$1° \times 1/3°$	NCEP/NCAR reanalysis	Griffies *et al.* (2005)
POP, LANL/NCAR	1960–2000	$1.125° \times 1/4°$	NCEP/NCAR + satellite products	Collins *et al.* (2006)
Data Assimilations				
ECCO, MIT	1992–2004	$1° \times 1°$	NCEP/NCAR	Wunsch and Heimbach (2007)
GODAS, NOAA/CPC	1980–2005	$1° \times 1/3°$	NCEP/NCAR	Behringer (2007)
Coupled Models				
GFDL-CM2.1, GFDL, USA	100 years, 20c3m	$1° \times 1°$ (1/3°) L40	—	Delworth *et al.* (2006)
UKMO-HadGem1, Hadley Centre, UK	95 years, 20c3m	$1° \times 1°$ (1/3°) L40	—	Johns *et al.* (2004)
CCSM3, NCAR, USA	100 years, 20c3m	$1.1° \times 1.1°$ (0.27°) L40	—	Collins *et al.* (2006)
MIROC3.2(medres), CCSR/NIES/FRCGC, Japan	100 years, 20c3m	$1.4° \times 0.5°$ L43	—	Hasumi and Emori (2004)
IPSL-CM4, IPSL, France	100 years, 20c3m	$2° \times 1°$ L31	—	Marti *et al.* (2005)
CSIRO-Mk3.5, CSIRO, Australia	100 years, 20c3m	$1.9° \times 0.8°$ L31	—	Gordon *et al.* (2002)

4. Results

Here, we will focus on the mean values of the wind power, buoyancy power, and the APE produced in the tropical ocean by the aforementioned ocean and coupled models, and ocean data assimilations.

a. Wind power

The Southern Ocean is the main source of wind power for the global oceans, closely followed by the tropical oceans, as can be seen in the example of the MOM4 model

(Fig. 1a). In this particular model, the mean wind power for the global ocean is approximately 1.7 TW (1 TW $= 10^{12}$ Watts), with the whole tropical band (15S to 15N) making up 0.7 TW of this total. Values of the wind power calculated from geostrophic currents (Fig. 1b) are generally smaller and show large regions of negative wind power (that is, where the winds remove energy from the ocean general circulation). In contrast, the wind power from ageostrophic flows (i.e. Ekman flow) is always positive (Wang and Huang, 2004). In the equatorial region, using the full zonal velocity is necessary for estimating ocean energetics, since the geostrophic approximation is not valid in this region.

Further, we will confine our study to the tropical Pacific (black box in Fig. 1a), since it is the largest contributor to the tropical wind power. In MOM4 the tropical Pacific generates 0.4 TW of the wind power or roughly 60% of the total for all tropical oceans.

Our estimates of the total mean wind power generated in the tropical Pacific Ocean basin range from 0.2 to 0.4 TW in ocean-only models and data assimilations, to almost 0.6 TW in some coupled models (Fig. 2 and Table 2). There are two main factors that explain the variations in the wind power values: the strength of the wind stress used or simulated in the model, and the structure of the simulated surface currents (Fig. 3). The mean wind power is approximately equal to the product of these two variables (see Eq. 3). Therefore, we can consider the two terms separately for inter-model comparisons.

The overall spatial structure of the wind stress in each model is reasonably consistent, though the magnitudes are not (Fig. 4, middle panels). Details of the wind stress curl are also different between the models, which becomes significant for the surface currents, and we will discuss this next. MOM and ORCAa are both forced with NCEP/NCAR reanalysis winds. POP uses an adjusted version of NCEP/NCAR wind stress (around 30% weaker, Maltrud and McClean, 2005). ECCO wind stress in the tropics displays a lot more meridional variability than the others, which can be explained in part by its shorter time span (13 years at the moment of writing, see Fig. 4c.) Even though all the models base their wind stress on either NCEP or ERA40 wind products, subsequent modifications employed by model developers result in noticeable differences in the wind forcing. The coupled models show even larger differences in wind stress (Fig. 4c,d), with some models simulating much stronger wind stress along the equator, in particular, the HadGEM model.

The meridional distribution of wind power closely aligns with the surface currents (compare Fig. 2 with Fig. 3 and Fig. 4 top panels with bottom panels). In particular, the wind power depends on the strength and size of the westward flowing South Equatorial Current (SEC), and the resolution of the eastward flowing North Equatorial Counter Current (NECC). The SEC flows in the same direction as the wind stress and so increases the wind power, while the NECC flows against the direction of the wind stress, decreasing the wind power.

All models/data assimilations have problems in simulating these currents, as compared to existing observations (Fig. 3, bottom). MOM and ORCAa have too broad SECs and little evidence of a NECC, leading to high values of wind power. The POP and ORCAb models and the data assimilations have a narrower SEC and a stronger NECC, leading to lower
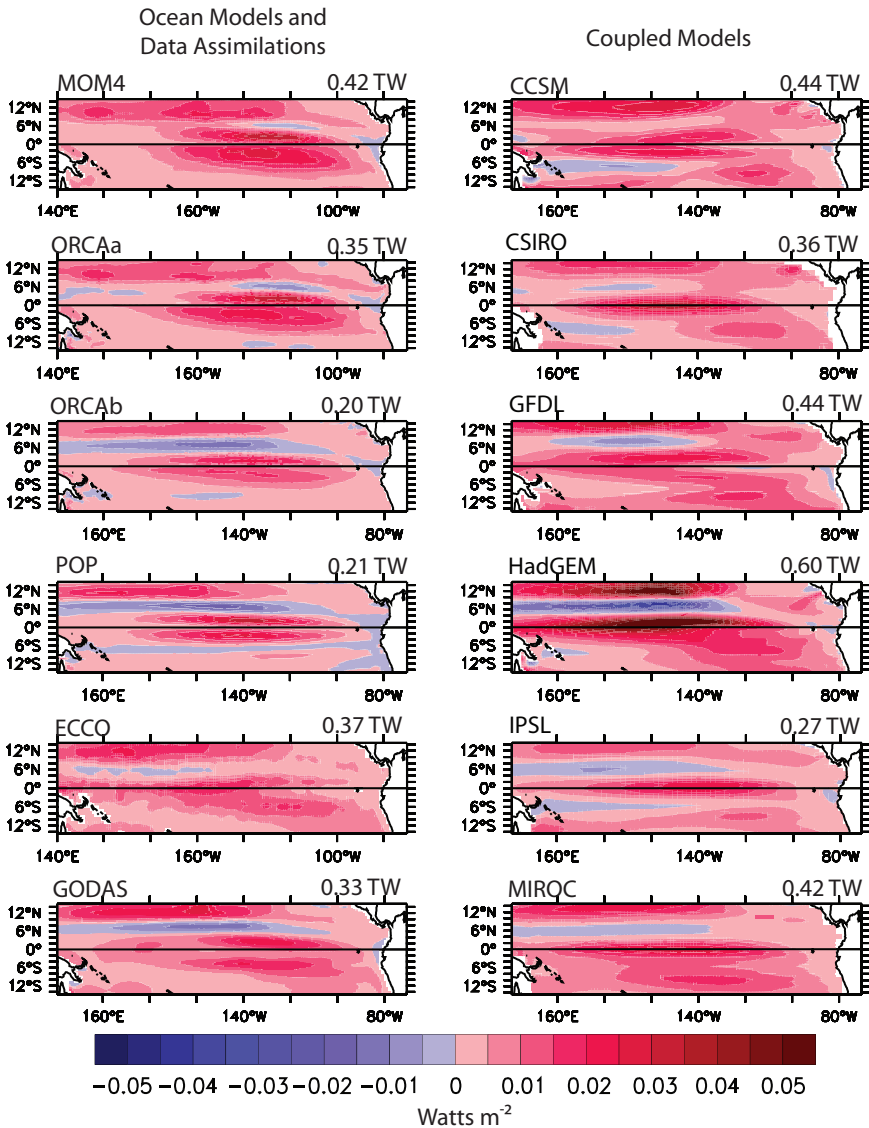
Figure 2. Mean wind power per unit area in the tropical Pacific for the ocean-only models, data assimilations, and coupled models, Watts m^{-2}. The wind power integrated over the whole region is given in the top right of each plot, in TW (terawatts).

wind power. Resolving the NECC correctly is important for obtaining realistic wind power in the tropics. In this case, POP and ORCAb perform the best.

The ORCAa and ORCAb runs make for an interesting comparison. These are largely the same models, but forced with different wind stress products. In ORCAa, a greater total

Table 2. Mean values of wind work, buoyancy work, the ratio of the two, and APE.

Model/data product	Wind work (TW)	Buoyancy work (TW)	B/W	APE (10^{18} J)
Ocean Models				
ORCAa	0.35	0.056	16%	4.7
ORCAb	0.20	0.037	19%	3.6
MOM4	0.42	0.062	15%	4.5
POP	0.21	0.025	12%	2.1
Data Assimilations				
ECCO	0.37	0.065	18%	1.8
GODAS	0.33	0.019	6%	2.5
Coupled Models				
GFDL-CM2.1,	0.44	0.056	13%	3.7
UKMO-HadGem1,	0.60	0.082	14%	4.6
CCSM3,	0.44	0.065	15%	4.0
MIROC3.2(medres),	0.42	0.053	13%	3.1
IPSL-CM4,	0.27	0.048	18%	1.5
CSIRO-Mk3.5,	0.36	0.059	16%	3.7

wind power (0.35 compared to 0.20 TW) is partially explained by the stronger wind stress applied. Differences in the surface currents of the two models, particularly how well they reproduce the NECC (Fig. 3), also contribute to the discrepancy. The particular expression of the NECC at the surface is generated by a complex interplay of the wind stress, wind stress curl and dynamical nonlinear effects, ultimately related to the different wind products used to force the models.

Decadal variability introduces further complications in estimating the wind power. While the coupled models have reasonably constant long-term means, the ocean-only products exhibit a clear reduction in the wind power in the late 1970s (Fig. 5, top). The decrease in wind power transfers to a decrease in available potential energy (Fig. 5, bottom), which is accompanied by a decrease in the thermocline slope at the same time (Guilderson and Schrag, 1998). How much of this decrease is caused by inaccuracies in the wind forcing before the 1980s and how much is caused by an actual weakening of the winds (discussed in Vecchi *et al.*, 2006, for example) remains to be seen. Encouragingly, the interannual variability in wind power is remarkably similar between the models (Fig. 5). This variability is discussed in Brown and Fedorov (2008), who look at the energetics of ENSO.

The coupled models considered in this study also present a broad range of results. At the low end, weak surface currents in the IPSL model lead to a small value of wind power. In HadGEM, both the NECC and the SEC are too strong, but the latter dominates in wind power calculations. This factor, combined with an exceptionally strong wind stress in HadGEM, leads to the highest estimate of wind power at 0.6 TW.

Where does the greater fraction of the wind power go? Analyzing the kinetic energy equation (see the Appendix) shows that the largest factor in energy loss is energy dissipation caused by friction in the equatorial currents with strong vertical and horizontal shear, including
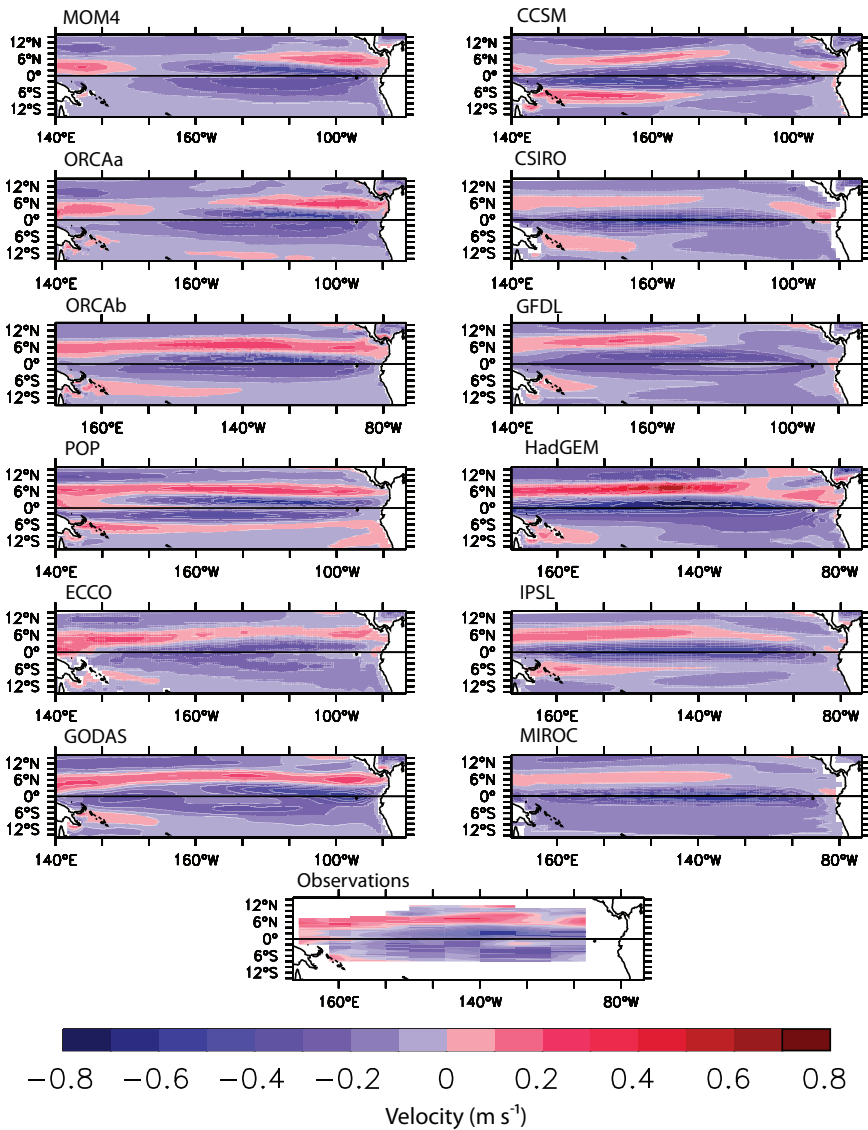
Figure 3. Mean surface currents (m s^{-1}) for each of the four ocean-only models, two data assimilations, six coupled model runs and available observations (observational data from Johnson *et al.*, 2002).

surface currents. In fact, roughly one half of the total wind power in the tropical ocean is related to surface ageostrophic flows (calculated as the difference between Figs. 1a and b) and is dissipated in the ocean mixed layer (Wang and Huang, 2004). A smaller, but still significant portion of the wind power is converted to buoyancy power, as discussed next.
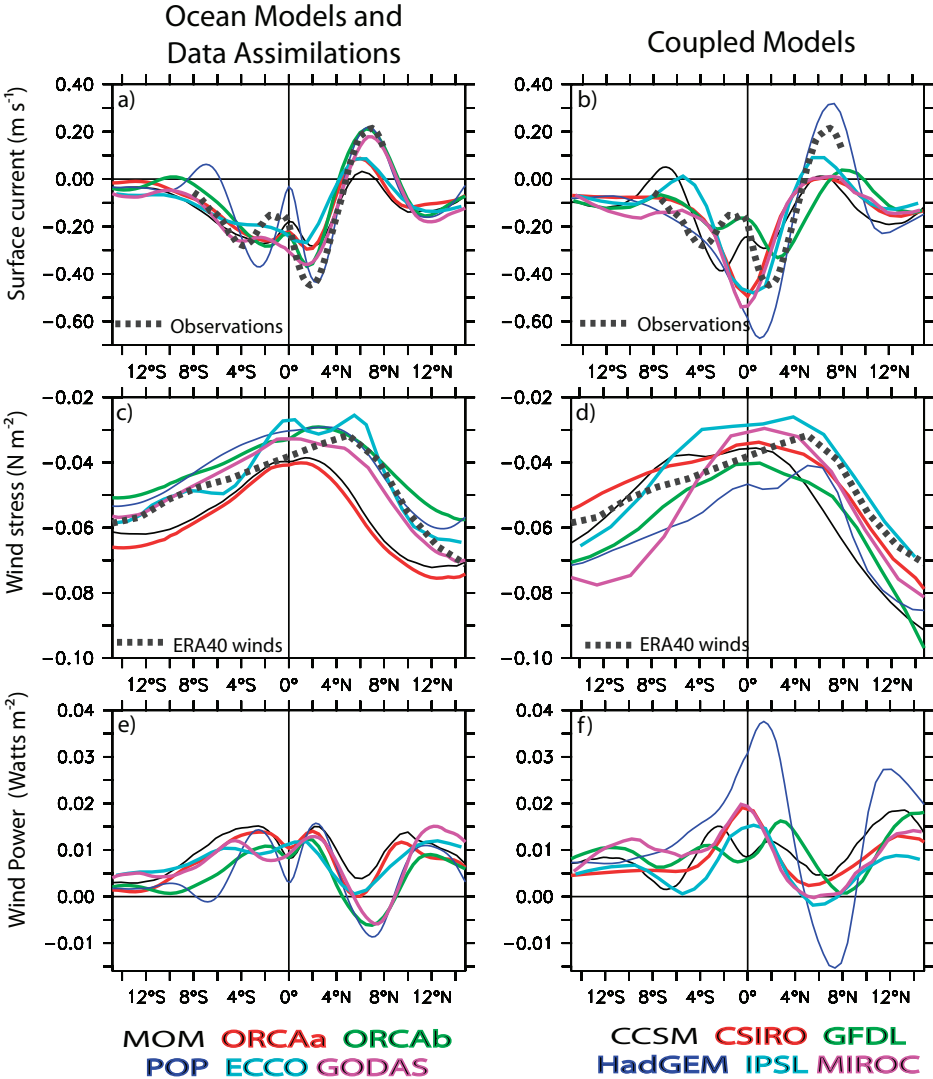
Figure 4. Zonal averages of the mean zonal velocity at the surface, mean wind stress, and mean wind power. The averaging is done from 160E to 90W to be consistent with the available observations of zonal currents.

b. Buoyancy power and available potential energy

Buoyancy power (Eq. 1), a result of the wind power conversion, transfers the energy from the winds into the interior of the ocean and induces vertical displacements of the isopycnals and hence changes in the APE. Values of mean buoyancy power in the models and data assimilations vary from 0.02 to 0.08 TW (Fig. 6). Even though the wind power acts on the
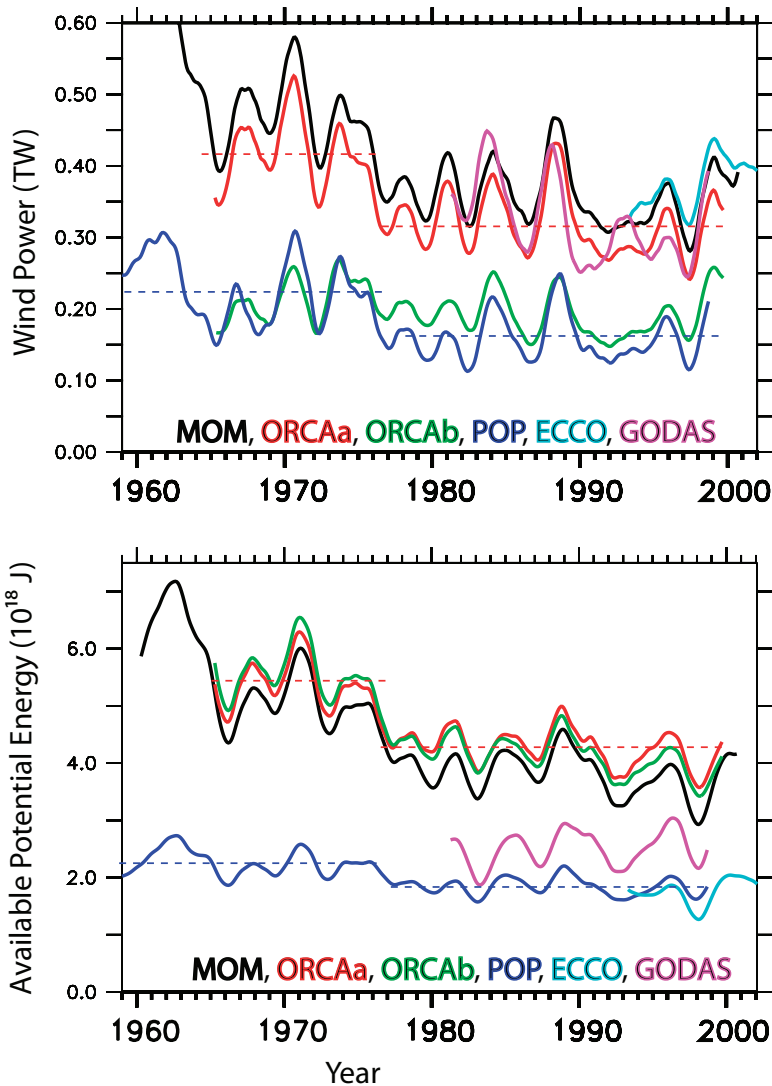
Figure 5. Time series of the wind power (top) and APE (bottom) for the ocean-only models and data assimilations showing a reduction in the wind power and the APE in the late 1970's. The magnitudes of the wind power and the APE vary significantly from one model to the next. Wind power is in TW (terawatts), the APE is Joules x10^{18}; a 31-point triangle filter was applied to the timeseries to remove annual and higher-frequency variations.

whole tropical Pacific region, in most cases the buoyancy power is primarily confined to within just a few degrees from the equator and to the eastern part of the basin. As buoyancy power is a function of vertical velocity, it is not surprising that it is strongest along the equator.
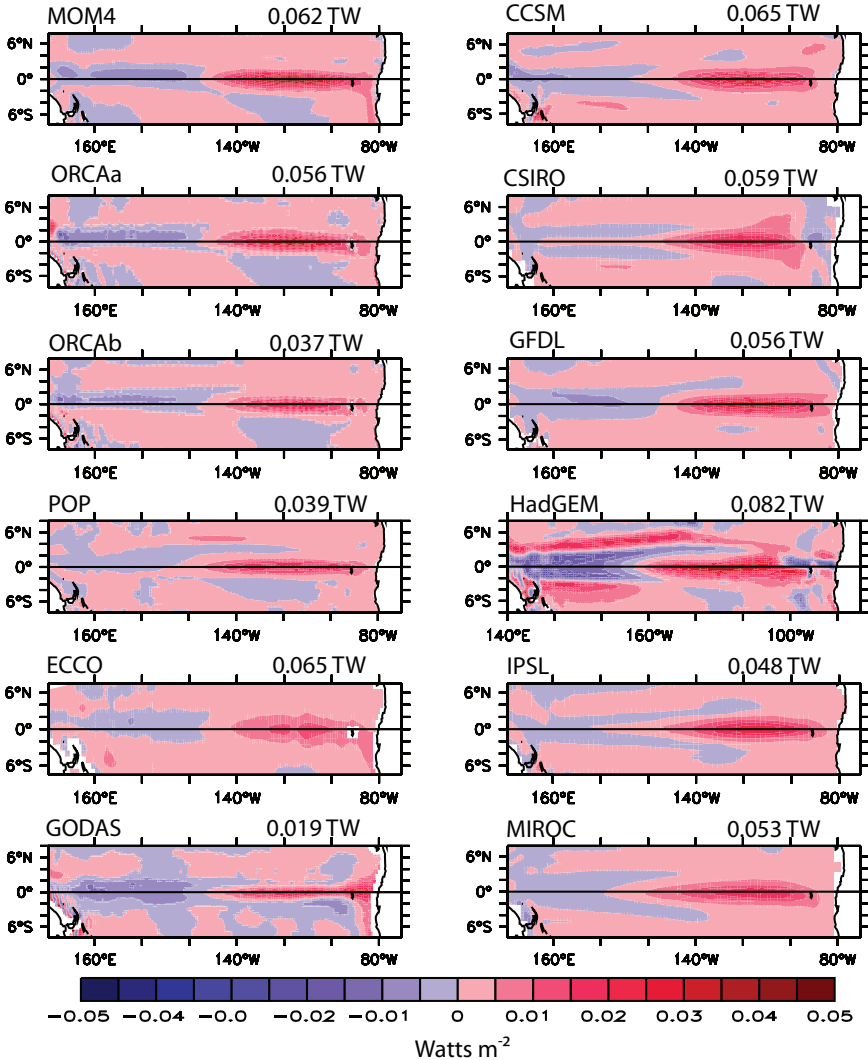
Figure 6. Mean buoyancy power per unit area ($\tilde{\rho}gw$) for each of the four ocean model runs, two data assimilations, and six coupled model runs, in Watts m^{-2}. The buoyancy power integrated over the whole region is given in the top right of each plot, in TW (terawatts).

In general, there is a good correlation between the magnitude of the wind power and the magnitude of the resulting buoyancy power on the ocean - a larger mean wind power usually implies a larger mean buoyancy power (Fig. 7a). Further, in the models and data assimilations we analyzed, roughly 10 to 20% of the wind power is converted to buoyancy power, depending on the model (excluding the GODAS data, see Fig. 7a and Table 2). The
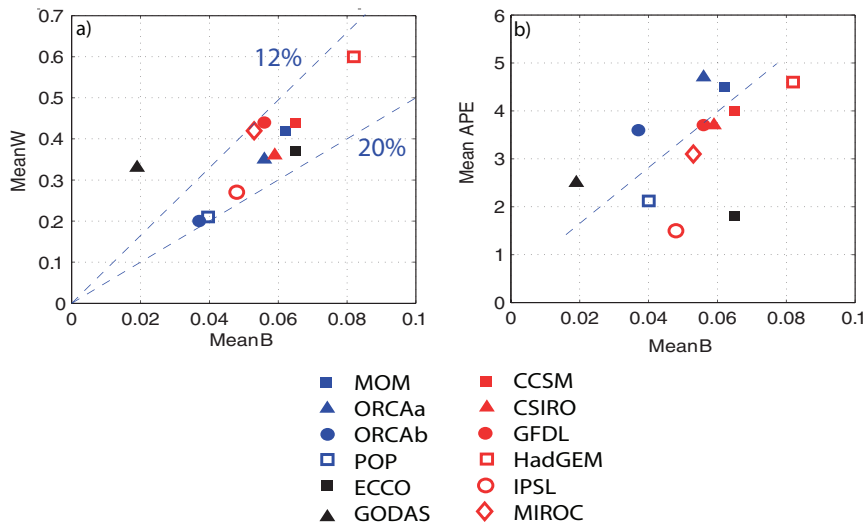
Figure 7. (a): Comparison of mean wind power (W) with mean buoyancy power (B). (b): Comparison of mean available potential energy (APE) with buoyancy power. Blue symbols show ocean only models, black symbols are data assimilations, and red symbols are coupled models. Units are TW (terawatts) for buoyancy and wind power, and Joules x 10^{18} for available potential energy. Note that only 12 to 20% of the wind power is converted to buoyancy power.

outlying value for GODAS can probably be accounted for by the fact that this data assimilation is not constrained by energy conservation.

In the mean sense, the buoyancy power can be considered as the fraction of the wind power required to maintain a constant APE associated with the mean slope of the thermocline (Fig. 7b). In other words, it is the power required to overcome the natural thermocline dissipation. In particular, this implies that the models with large values of buoyancy power (e.g. HadGEM) have a more dissipative thermocline.

Thus, the generated buoyancy power is essential for maintaining the mean slope of the isopycnals, particularly the thermocline slope along the equator, and balancing the gradual dissipation of the APE. Analyzing the APE equation (see the Appendix) suggests that the main factors in this energy dissipation are model vertical and horizontal diffusion, the advection of the APE away from the tropics, and energy damping by surface heat fluxes.

Typically, a larger mean buoyancy power leads to a larger mean APE in the model, even though the correlation between the two variables is not very strong (Fig. 7b). Finally, that the mean APE in the tropical Pacific is a measure of the thermocline slope becomes clear from Figure 8b. Models with a stronger thermocline tilt and a larger APE usually have a deeper equatorial thermocline (Fig. 8a).
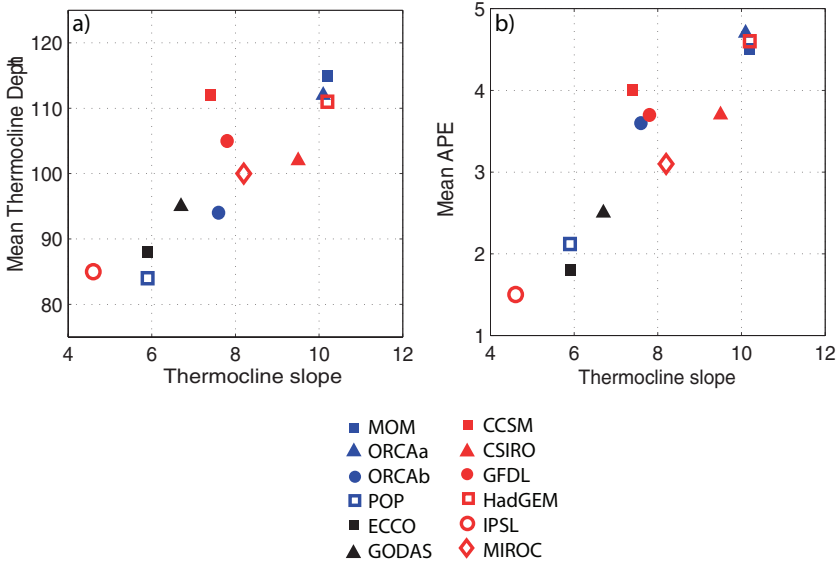
Figure 8. Comparison of mean thermocline depth, mean thermocline slope and mean APE. The thermocline slope is defined as the normalized difference between thermocline depth at 180E and 100W, where an appropriate isopycnal was chosen for each individual model. The mean thermocline depth is defined as the depth of where $d\rho/dz$ is maximum. In POP and HadGEM however, this depth was not clearly defined and so the depth of an appropriate isopycnal was used.

5. Discussion and conclusions

Our estimates of mean wind power acting on the tropical Pacific Ocean, based on ocean-only models and data assimilations, range from 0.2 to 0.4 TW (Fig. 2). Furthermore, these models exhibit a weak to moderate decrease in the wind power over the last 50 years (Fig. 5) so that the values of the wind power actually depend on the averaging interval.

Why are these estimates so different? Which estimates are more trustworthy? The values of the mean wind power depend primarily on how well the models reproduce the mean surface ocean currents, and on the strength and spatial structure of the winds they are forced with (Fig. 4). There are indications that the ERA-40 wind stress product may be closer to observations in the tropics than the NCEP wind stress (Caires *et al.*, 2004). Nevertheless, there is still a large uncertainty in the winds, which is reflected in the differences between the forcing used by different research groups. Similarly there are considerable variations between the meridional structure of the modeled ocean currents and that of the observations.

The estimates of wind power can be broadly categorized into two groups: those forced with NCEP reanalysis winds (MOM, ORCAa, ECCO and GODAS) and those forced with other products (ORCAb and POP) closer to the ERA-40 wind stress. The NCEP winds produce a stronger mean wind power of 0.33 to 0.42 TW, while the others are weaker at

around 0.2 TW. The ORCA models (a and b) are examples of the same model, forced with different winds, generating very different wind power. Identifying which results are more accurate will require a combination of better ocean models, high-quality observations of ocean surface currents, and, especially, more reliable estimates of the wind stress.

The coupled models analyzed in this study also produce a broad range of results for mean wind power - from 0.3 TW to 0.6 TW. The discrepancies are caused by even larger differences in the simulated wind stress and surface currents as compared to the ocean-only models and data assimilations (Fig. 4).

It is clear that correctly resolving equatorial surface currents in models should be an important consideration in the ocean energetics. In particular, the extent and magnitude of the South Equatorial Current and the surface expression of the North Equatorial Counter Current are key in determining the amount of wind power generated in the tropical Pacific Ocean. In fact, these currents are as important in calculating the total energy balance of the ocean as other major oceanic currents, such as the Antarctic Circumpolar Current and the Gulf Stream.

The decrease in the mean wind power in the tropical Pacific over the last 50 years has resulted in a reduction of the ocean available potential energy, which indicates a reduction in the thermocline tilt over the same time interval (Fig. 5). This flattening of the thermocline occurred around the time of the climate regime-shift in the late 1970s (Guilderson and Schrag, 1998) and is associated with a weakening of the zonal winds along the equator (Vecchi *et al.*, 2006). A flatter thermocline can lead to stronger El Niño events (Fedorov and Philander, 2000, 2001).

The decrease in the wind power in the tropics is opposite to the trends in the global mean power. Over the last 25 years, the global wind energy input to the surface currents has increased by approximately 12% (Huang *et al.,* 2006), but most of this increase has occurred in the Southern Ocean.

Roughly 10 to 20% of the wind power in the tropics is converted to buoyancy power needed to replace energy lost from the thermocline. It is interesting that the upper bound is close to the commonly used efficiency of the conversion of the turbulent kinetic energy of oceanic flows into gravitational potential energy via turbulent mixing (the "mixing efficiency" usually estimated at 20%, see Osborn, 1980; Wunsch and Ferrari, 2004). The turbulent mixing raises the center of mass of a localized system and increases its potential energy.

Energy balances in the tropical Pacific are also crucial for the El Niño Southern Oscillation phenomenon because they affect the thermocline tilt along the equator. In Brown and Fedorov (2008) we extend our approach to explore interannual variability in the tropics and describe ENSO in terms of wind power, buoyancy power and APE transformations. We argue that understanding how energy is transferred from the winds to the ocean thermocline during a La Niña - El Niño cycle is critical for understanding differences between the model's simulations of ENSO.

Ultimately, wind power in the tropics is only one piece of a complex total energy budget of the ocean of which much is yet to be learnt. One of the challenging issues, for

example, is how much mechanical energy from winds, tides and perhaps other sources is necessary for ocean turbulent mixing to maintain the upwelling of cold water to the ocean surface against the deep ocean stratification (Wunsch and Ferrari, 2004; Munk and Wunsch, 1998).

APPENDIX

Derivation of the energy equations

The kinetic energy equation

We begin with the horizontal momentum equations,

$$u_t + \boldsymbol{u} \cdot \nabla u - fv = -\frac{p_x}{\rho} + (\kappa_{MH}u_x)_x + (\kappa_{MH}u_y)_y + (\kappa_{MV}u_z)_z, \text{ and}$$

$$v_t + \boldsymbol{u} \cdot \nabla v + fu = -\frac{p_y}{\rho} + (\kappa_{MH}v_x)_x + (\kappa_{MH}v_y)_y + (\kappa_{MV}v_z)_z,$$

(7)

where $\boldsymbol{u} = (u,v,w)$ is the 3-D velocity field, p is pressure, ρ is density, $\tau = (\tau^x, \tau^y)$ is wind stress and κ_{MV} and κ_{MH} are the vertical and horizontal eddy viscosities, respectively. The boundary conditions are

$$\kappa_{MV}u_z\big|_{z=0} = \frac{\tau^x}{\rho}, \quad \kappa_{MV}v_z\big|_{z=0} = \frac{\tau^y}{\rho},$$

$$u, v \rightarrow 0 \text{ as } z \rightarrow -\infty.$$

(8)

By multiplying the zonal momentum equation by u, and multiplying the meridional momentum equation by v, adding the two, and integrating over the volume of the tropical basin, one obtains

$$\frac{\partial K}{\partial t} = W - B - P - A_M - D_M \tag{9}$$

where

$$K = \iiint \hat{K}dV = \iiint \frac{\rho_0}{2}(u^2 + v^2)dV$$

$$W = \iint \boldsymbol{v} \cdot \boldsymbol{\tau}dS$$

$$B = \iiint \tilde{\rho}gwdV$$

$$P = \oint (p + p_s)\boldsymbol{u} \cdot \boldsymbol{n}d\sigma \tag{10}$$

$$A_M = \oint \hat{K}\boldsymbol{u} \cdot \boldsymbol{n}d\sigma$$

$$D_M = \iiint \kappa_{MV}(\boldsymbol{v}_z \cdot \boldsymbol{v}_z)dV + \iiint \kappa_{MH}[(\boldsymbol{v}_x \cdot \boldsymbol{v}_x) + (\boldsymbol{v}_y \cdot \boldsymbol{v}_y)]dV$$

with W the wind power, B the buoyancy power, and P the change in kinetic energy due to work done against pressure gradients by the ageostrophic flow. A_M is the flux of kinetic energy through the walls of the tropical basin due to advection, and D_M is the energy dissipation due to friction induced by vertical and horizontal shear in the equatorial currents (i.e. viscous dissipation).

Note that here $\boldsymbol{v} = (u,v)$ are the horizontal components of current velocity. The wind power is integrated over the surface of the tropical basin; other variables are integrated over the volume V or the walls of the basin boundary σ. Other terms are p_s - sea level pressure, $\boldsymbol{n}$ unit vector out of the region. Potential density is given by $\tilde{\rho} = \rho - \rho^*$, with ρ^* being a horizontal average over the basin of interest (Fig. 1a), and ρ_0 - the mean background density.

The available potential energy equation

For this study we define the available potential energy (APE) as done in Margules (1905) and Lorenz (1955). In this definition the APE is the difference between the total potential energy of a fluid and the potential energy of the same fluid mass in the same basin after an isentropic adjustment to a stable, exactly hydrostatic, reference state in which the isosteric and isobaric surfaces are level (Reid *et al.*, 1981).

The APE or just E for brevity (measured in Joules), is calculated in terms of density, according to Oort *et al.* (1989) as

$$E = \iiint \hat{E} dV = \iiint \frac{1}{2} \frac{\tilde{\rho}^2}{S^2} \, dV. \tag{11}$$

A stability factor S is introduced as $S^2 = |\rho_z^*/g|$, which differs from the buoyancy frequency by a factor of g^2/ρ^*. A derivation of this expression for the APE and its limitations can be found in Huang (1998) and Huang (2005).

The derivation of the APE balance begins with the density equation, which is a consequence of the advection-diffusion equations for temperature and salt, with the same temperature and salt diffusivities, and a linear equation of state of sea water (Goddard and Philander, 2000).

$$\tilde{\rho}_t + \boldsymbol{u}\nabla\tilde{\rho} + w\rho_z^* = \kappa_{TH}(\tilde{\rho}_{xx} + \tilde{\rho}_{yy}) + [\kappa_{TV}(\rho_z^* + \tilde{\rho}_z)]_z + Q_\rho \tag{12}$$

where Q_ρ describes the effect of thermal and freshwater fluxes in the upper few layers of the model so that $Q_\rho = -\alpha_0 Q_{heat} + \beta_0 Q_{salt}$. The linear equation of state for sea water is written as $\rho = \rho_0 - \alpha_0 T + \beta_0 S$, while κ_{TH} and κ_{TV} are the horizontal and vertical eddy diffusivities.

Potentially, one can use a nonlinear equation of state for sea water and different diffusivities for salt and temperature (think double diffusion). In that case, the right-hand side of Eq. (12) will acquire several additional terms which will eventually give rise to additional sources and sinks of energy in the APE equation. However, for the very narrow range of temperature and salinity changes in the tropical ocean above 400 m, the errors of the linearized equation of state do not exceed more than a few percents (Goddard, 1995). Nor would one expect big differences, if any, between eddy salt and temperature diffusivities for the large-scale motion in the tropical ocean.

Using Eq. (12), Goddard and Philander then derive the rate of change of the available potential energy to be:

$$\frac{\partial E}{\partial t} = B - Q - A - D \tag{13}$$

$$Q = -\iiint \left(\frac{\tilde{\rho}}{S^2} Q_\rho\right) dV$$

$$A = \oiint (\boldsymbol{u}\hat{E}) \cdot \boldsymbol{n} d\sigma \tag{14}$$

$$D = -\iiint \hat{E} w \left(\frac{\rho_{zz}^*}{\rho_z^{*2}}\right) dV - \oiint \kappa_{TH}\nabla\hat{E} \cdot (\hat{\imath}, \hat{\jmath}) d\sigma$$

$$+ \iiint \frac{\kappa_{TH}}{S^2} [(\tilde{\rho}_x)^2 + (\tilde{\rho}_y)^2] dV - \iiint \left(\frac{\tilde{\rho}}{S^2} (\kappa_{TV}(\tilde{\rho} + \rho^*)_z)_z\right) dV$$

where B is the buoyancy power, A is the energy advection through the region boundary, and D is the total energy dissipation due to processes associated with vertical and horizontal diffusion (i.e. diffusive dissipation) and with shear in the stability profile. Q describes the effect of thermal and freshwater sources at the surface on the density field (with heat fluxes dominating). The vertical integration for Q_ρ should be conducted over the few upper layers of the model.

Further details of the energy balance in the tropical Pacific can be found in Goddard and Philander (2000), and are discussed in Griffies (2004), Chapter 5.

REFERENCES

Behringer, D. W. 2007. The Global Ocean Data Assimilation System at NCEP. 11th Symposium on Integrated Observing and Assimilation Systems for Atmosphere,Oceans,and Land Surface, AMS 87th Annual Meeting, Henry B. Gonzales Convention Center, San Antonio, TX, 12 pp.

Barnier, B., G. Madec, T. Penduff, J. M. Molines, A. M. Treguier, J. Le Sommer, A. Beckmann, A. Biastoch, C. Boning, J. Dengg, C. Derval, E. Durand, S. Gulev, E. Remy, C. Talandier, S. Theetten, M. Maltrud, J. McClean and B. De Cuevas. 2006. Impact of partial steps and momentum advection schemes in a global ocean circulation model at eddy-permitting resolution. Ocean Dyn., *56*, 543-567.

Brown, J. N. and A. V. Fedorov. 2008. Energy transfer from the winds to the thermocline on ENSO timescales. (in preparation).

Caires, S., A. Sterl, J.-R. Bidlot, N. Graham and V. Swail. 2004. Intercomparison of different wind-wave reanalyses. J. Climate, *17*, 1893-1913.

Collins, W. D., C. M. Bitz, M. L. Blackmon, G. B. Bonan, C. S. Bretherton, J. A. Carton, P. Chang, S. C. Doney, J. J. Hack, T. B. Henderson, J. T. Kiehl, W. G. Large, D. S. McKenna, B. D. Santer, and R. D. Smith. 2006. The Community Climate System Model Version 3 (CCSM3). J. Climate, *19*, 2122-2143.

Delworth, T. L. and Coauthors. 2006. GFDL's CM2 global coupled climate models. Part I. Formulation and simulation characteristics. J. Climate, *19*, 643-674.

Fedorov, A.V. 2007. Net energy dissipation rates in the tropical ocean and ENSO dynamics. J. Climate, *20*, 1099–1108.

Fedorov, A. V., S. L. Harper, S. G. Philander, B. Winter and A. T. Wittenberg. 2003. How predictable is El Nino? Bull. Amer. Meteor. Soc., *84*, 911-919.

Fedorov, A.V. and S.G. Philander. 2001. A stability analysis of the tropical ocean-atmosphere interactions. Bridging Measurements of, and Theory for El Niño. J. Climate, *14*, 3086-3101.

——2000. Is El Niño changing? Science, *288*, 1997-2002.

Goddard, L. and S. G. Philander. 2000. The energetics of El Nino and La Nina. J. Climate, *13*, 1496-1516.

Gordon, H. B., L. D. Rotstayn, J. L. McGregor, M. R. Dix, E. A. Kowalczyk, S. P. O'Farrell, A. C. Hirst, S. G. Wilson, M. A. Collier, I. G. Watterson and T. I. Elliot. 2002. The CSIRO Mk3 Climate System Model. Electronic publication. Aspendale. CSIRO Atmospheric Research. (CSIRO Atmospheric Research Technical Paper; no. 60) 130 pp.

Griffies, S. M. 2004. Fundamentals of Ocean Climate Models, Princeton University Press, 518 + xxxiv pp.

Griffies, S. M., A. Gnanadesikan, K. W. Dixon, J. P. Dunne, R. Gerdes, M. J. Harrison, A. Rosati, J. Russell, B. Samuels, M. J. Spelman, M. Winton and R. Zhang. 2005. Formulation of an ocean model for global climate simulations. Ocean Sci., *1*, 45-79.

Guilderson, T. and D. P. Schrag. 1998. Abrupt shift in subsurface temperatures in the Tropical Pacific associated with changes in El Nino. Science, *281*, 240-243.

Hasumi, H. and S. Emori. (Eds.) 2004. K-1 coupled model (MIROC) description. K-1 Tech. Rep. 1, Center for Climate System Research, University of Tokyo. 34 pp.

Huang, R. X. 2005. Available potential energy in the world's oceans. J. Mar. Res., *63*, 141-158.

——2004. Ocean, Energy Flow, *in* Encyclopedia of Ocean Sciences, *4*, 497-509.

——1998. Mixing and available potential energy in a Boussinesq Ocean. J. Phys. Oceanogr. *28*, 669-678.

Huang, R. X., W. Wang and L. L. Liu. 2006. Decadal variability of wind-energy input to the world ocean. Deep-Sea Res. II, *53*, 31-41.

Johns, T. and Coauthors. 2004. HadGEM1 - Model description and analysis of preliminary experiments for the IPCC Fourth Assessment Report. Tech Rep. *55*, Met Office, Exeter, United Kingdom.

Johnson, G. C., B. M. Sloyan, W. S. Kessler and K. E. McTaggart. 2002. Direct measurements of upper ocean currents and water properties across the tropical Pacific during the 1990s. Prog. Oceanogr., *52*, 31-61.

Lorenz, E. N. 1955. Available potential energy and the maintenance of the general circulation. Tellus, VII, 157-167.

Maltrud, M. E. and J. L. McClean. 2005. An eddy resolving global 1/10 degrees ocean simulation. Ocean Model., *8*, 31-54.

Maltrud, M., J. L. McClean and B. De Cuevas. 2006. Impact of partial steps and momentum advection schemes in a global ocean circulation model at eddy-permitting resolution. Ocean Dyn., *56*, 543-567.

Margules, M. 1905. Uber die energie der sturme. Wein. K. K. Hot-und. Stattsdruckerei, 26 pp Marti, O. and Coauthors. 2005. The new IPSL climate system model. IPSL-CM4., Institut Pierre Simon Laplace des Sciences de l'Environment Global, IPSL, Case 101, Paris, France.

Meehl, G., D. Covey, T. L. Delworth, M. Latif, B. McAvaney, J. F. B. Mitchell, R. J. Stouffer and K. E. Taylor. 2007. The WRCP CMIP3 Multimodel Dataset. BAMS, 1383-1394.

Munk, W. and C. Wunsch. 1998. Abyssal recipes II. energetics of tidal and wind mixing. Deep-Sea Res. I, *45*, 1977-2010.

Oort, A. H., S. C. Ascher, S. Levitus and J. H. Peixoto. 1989. New estimates of the available potential energy in the world ocean. J. Geophys. Res., *94*, 3187-3200.

Osborn, T. R. 1980. Estimates of the local rate of vertical diffusion from dissipation measurements. J. Phys. Oceanogr., *10*, 83-89.

Reid, R. O., B. A. Elliot and D. B. Olson. 1981. Available potential energy: A Clarification. J. Phys. Oceanogr, *11*, 15-29.

Uppala, S. M., P. W. Kallberg, A. J. Simmons, U. Andrae, V. D. Bechtold, M. Fiorino, J. K. Gibson, J. Haseler, A. Hernandez, G. A. Kelly, X. Li, K. Onogi, S. Saarinen, N. Sokka, R. P. Allan, E. Andersson, K. Arpe, M. A. Balmaseda, A. C. M. Beljaars, L. Van De Berg, J. Bidlot, N. Bormann, S. Caires, F. Chevallier, A. Dethof, M. Dragosavac, M. Fisher, M. Fuentes, S. Hagemann, E. Holm, B. J. Hoskins, L. Isaksen, P. Janssen, R. Jenne, A. P. McNally, J. F. Mahfouf, J. J. Morcrette, N. A. Rayner, R. W. Saunders, P. Simon, A. Sterl, K. E. Trenberth, A. Untch, D. Vasiljevic, P. Viterbo, and J. Woollen. 2005. The ERA-40 re-analysis. Quar. J. Royal Met. Soc., *131*, 2961-3012.

Vecchi, G., B. J. Soden, A. T. Wittenberg, I. M. Held, A. Leetmaa and M. J. Harrison. 2006. Weakening of the tropical Pacific atmospheric circulation due to anthropogenic forcing. Nature, *441*, 73-76.

Wang, W. and R. X. Huang. 2004. Wind energy input to the Ekman layer. J. Phys. Oceanogr., *34*, 1267-1275.

Weijer, W. and S. T. Gille. 2005. Energetics of wind-driven barotropic variability in the Southern Ocean. J. Mar. Res., *63*, 1101-1125.

Wunsch, C. 1998. The work done by the wind on the oceanic general circulation. J. Phys. Oceanogr., *28*, 2332-2340.

Wunsch, C. and R. Ferrari. 2004. Vertical mixing, energy, and the general circulation of the oceans. Annu. Rev. Fluid. Mech., *36*, 281-314.

Wunsch, C. and P. Heimbach. 2007. Practical global ocean state estimation. Physica D, *230*, 197-208.